Effect of the IrO$_x$ Conductivity on the Anode Electrode/Porous Transport Layer Interfacial Resistance in PEM Water Electrolyzers

M. Bernt,[1,2,z,a] C. Schramm,[1] J. Schröter,[1,2] C. Gebauer,[3] J. Byrknes,[4] C. Eickes,[4] and H. A. Gasteiger[1]

[1]*Chair of Technical Electrochemistry, Department of Chemistry and Catalysis Research Center, Technische Universität München, 85748 Garching, Germany*
[2]*Bayerisches Zentrum für Angewandte Energieforschung, 85748 Garching, Germany*
[3]*Heraeus Deutschland GmbH & Co. KG, Heraeus Precious Metals, 63450 Hanau, Germany*
[4]*Greenerity GmbH, 63457 Hanau-Wolfgang, Germany*

In this study, a commercial IrO$_2$/TiO$_2$ catalyst (75 wt% Ir, named "Benchmark") for the oxygen evolution reaction (OER) is compared to a newly developed IrO(OH)$_x$/TiO$_2$ catalyst (45 wt% Ir, named "P2X"). Due to its lower Ir packing density and higher OER activity vs the Benchmark catalyst (440 vs 12 A g$_{Ir}^{-1}$ at 1.43 V$_{iR\text{-free}}$), the P2X catalyst shows an improved PEM (proton exchange membrane) water electrolyzer performance at ≈9 times reduced Ir loading, however, only if a platinum-coated porous transport layer (PTL) at the anode is used. While the performance of membrane electrode assemblies (MEAs) with the Benchmark catalyst is unaffected when using an untreated titanium PTL, MEAs with the P2X catalyst perform poorly, which can be attributed to a contact resistance at the anode/PTL interface due to the low electrical conductivity of the P2X catalyst (0.7 S cm^{-1}) vs the Benchmark catalyst (416 S cm^{-1}) and the passivation of the Ti-PTL. A heat treatment procedure is used to transform the amorphous IrO(OH)$_x$ of the P2X catalyst into crystalline IrO$_x$ and, hence, increases its electrical conductivity. The optimum temperature for heat treatment to maximize electrical conductivity, OER activity and MEA performance will be evaluated.
© 2021 The Author(s). Published on behalf of The Electrochemical Society by IOP Publishing Limited. This is an open access article distributed under the terms of the Creative Commons Attribution 4.0 License (CC BY, http://creativecommons.org/licenses/by/4.0/), which permits unrestricted reuse of the work in any medium, provided the original work is properly cited. [DOI: 10.1149/1945-7111/ac1eb4]

Hydrogen as a medium for large-scale energy storage will become an important factor in a future energy scenario mainly based on renewable energy sources. Proton exchange membrane water electrolysis (PEM-WE) with its high power density and excellent load following capability seems to be a perfectly suited technology to facilitate hydrogen production from renewable electricity.[1] However, high investment costs still present a major challenge for a large-scale application of the technology.[2,3] Since costs for flow fields and separators, which up to now represented the major part of the stack costs, could recently be reduced by up to 80%, the membrane electrode assembly (MEA) is now the biggest cost contributor with ≈40% of the total stack costs.[4] Here, typically carbon-supported platinum catalysts (Pt/C) are used for the hydrogen evolution reaction (HER) on the cathode, while catalysts based on iridium (Ir) are used for the oxygen evolution reaction (OER) on the anode. Since catalyst loadings are still very high (several mg cm^{-2}),[1,4,5] a reduction of the catalyst loading, especially of the iridium loading on the anode, is of great importance to enable a large-scale application of PEM-WEs, not only because of the high costs of the catalyst materials, but also in the context of the limited availability of iridium.[5] Here it should be noted that the required platinum loadings on the cathode are comparatively negligible (⩽0.1 mg$_{Pt}$ cm^{-2}), due to the fast HER kinetics in the PEM environment.[6] In a recent study, we estimated that a reduction in iridium loadings from currently ≈2 mg$_{Ir}$ cm^{-2} to ≈0.05 mg$_{Ir}$ cm^{-2} would be required in order to allow installation capacities of ⩾100 GW year^{-1} that would be required for a global hydrogen economy based on H$_2$ generation by water electrolysis.[6,7]

A typical approach to enable lower anode catalyst loadings is to increase the activity of the OER catalyst and, consequently, most research in the field aims at finding materials that provide an improved mass activity for the OER compared to conventional iridium-based catalysts. Ruthenium or RuO$_x$ has a higher OER activity compared to Ir/IrO$_x$,[8,9] but is not sufficiently stable to be used as a catalyst in PEM-WEs.[10] Mixed Ir-Ru oxides have been proposed to combine the high activity of Ru with the high stability of Ir,[11] however, dissolution of the Ru species is still an issue.[12] For Ir based catalysts itself, a strong dependency of catalytic activity and oxidation state has been found.[13] Typically, amorphous IrO$_x$ with a high concentration of Ir^{3+} surface species shows a higher OER activity compared to crystalline IrO$_2$, which is usually prepared by calcination at higher temperatures.[14,15] To further increase the mass activity of Ir-based catalysts, core–shell structures, e.g., based on a dealloyed IrNi core with an IrO$_x$ shell concept or even more advanced structures, such as Ir-Ni two dimensional nanoframes[16,17] as well as Ir–Ni and Ir–Co nanowires have been proposed.[18] These catalysts show much higher mass activities compared to typical commercial Ir-based catalysts. However, most of the studies solely rely on measurements in model systems such as rotating disk electrodes (RDE) and the high mass activity obtained there does not guarantee a good performance at low Ir loadings in a real PEM-WE system.

When OER catalyst materials are used to fabricate MEAs for the use in an actual PEM-WE, besides of their OER activity, several other factors are critical to obtain high and stable performance. One factor is the requirement that no significant amount of transition metals are being leached from the catalyst, as they would ion exchange with the protons in the proton exchange membrane and deteriorate the PEM-WE performance,[19,20] particularly at higher current densities (note that this effect is absent in RDE measurements due to the large proton inventory in the electrolyte in this case).

A second factor are the structural properties of the catalyst that are critical to obtain a good performance at high current densities and, most importantly, at low iridium loadings. In a previous study, we identified the iridium packing density, i.e., the amount of iridium packed into a given catalyst layer volume (in units of g$_{Ir}$ cm$^{-3}_{electrode}$) as a crucial parameter to enable low Ir loadings.[6] Typical commercial Ir based catalysts have a high volume fraction of Ir and, consequently, low Ir loadings would result in extremely thin catalyst layers. For example, the commercial OER catalyst used as

[a]Present address: Freudenberg FST GmbH, Bayerwaldstr. 3, 81737 München, Germany.
[z]E-mail: maxbernt@freenet.de

benchmark in this study, viz., crystalline iridium oxide deposited as a thick layer on an electrically non-conductive titanium oxide support (c-IrO$_2$/TiO$_2$, with 75 wt% Ir from Umicore; furtheron referred to as "Benchmark" catalyst) has an iridium packing density of $\approx$2.3 g$_{Ir}$ cm^{-3}$_{electrode}$,[7] resulting in an electrode thickness of $\approx$9 μm at the typically used loading of 2 mg$_{Ir}$ cm^{-2}, while at Ir loadings of <0.5 mg$_{Ir}$ cm^{-2}, the electrodes are too thin (<2 μm) and inhomogeneous, which results in a significant performance drop.[6] Thus, while a kinetic analysis shows that a reduction of the Ir loading from 2 mg$_{Ir}$ cm^{-2} (used today) to the long-term target of 0.05 mg$_{Ir}$ cm^{-2} (required for a global H$_2$ economy where H$_2$ is produced by PEM-WE) would only incur a OER kinetic penalty of $\approx$80 mV, practically such low loadings cannot be realized.[6] This illustrates the importance of a low Ir packing density to reduce the Ir loading in a PEM-WE.

The third critical factor is the electrical conductivity of the catalyst, an important property which is often not taken into account when new catalysts are developed. A sufficient electrical conductivity is required for the transport of electrons to/from the active OER catalyst sites and across the thickness of the catalyst layer that is much thicker in a PEM-WE ($\approx$5 μm) than what is used in RDE experiments (typically less than $\approx$0.5 μm). Particularly when used in MEAs for a PEM-WE, a high electrical conductivity of the catalyst is also required: i) to reduce the contact resistance between the anode catalyst layer and the porous transport layer (PTL) at the anode side of a PEM-WE and ii) to assure a sufficiently small in-plane electrical resistance across the $\approx$10–20 μm wide pores in the PTL.[6] The contact resistance is particularly critical, if a pure titanium PTL without conductive coating is used, so that in some instances thin platinum coatings are applied to titanium PTLs to minimized this contact resistance.[4] Other approaches to improve the interface properties between catalyst layer and PTL include the fabrication of multilayer PTL structures with a reduced surface roughness compared to conventional PTLs[21] as well as the application of a IrO$_x$ nanofiber interlayer between PTL and catalyst layer.[22]

The electrical conductivity of iridium oxide strongly depends on its crystallinity: amorphous and/or hydrous iridium oxide have low electrical conductivities, but upon thermal annealing ($\approx$300 °C– 550 °C) of these materials to form crystalline iridium oxide, the electrical conductivity increases by several orders of magnitude.[23,24] At the same time, the OER activity of amorphous/hydrous iridium oxide is found to be at least an order of magnitude larger than that of crystalline iridium oxide.[14,15] While typical commercial OER catalysts use high loadings of crystalline iridium oxide (c-IrO$_2$) to provide good electrical conductivity, they currently suffer from high Ir packing densities that prevent their use at low iridium loadings in MEAs for PEM-WEs, as discussed above and in Ref. 6 low Ir packing densities could be achieved, if iridium oxide nanoparticles could be supported on a conductive support material, as is done for platinum based fuel cell catalysts that are supported on high surface area carbons (e.g., $\approx$0.08 g$_{Pt}$ cm^{-3}$_{electrode}$[6,7] for a 15 wt% Pt/C catalyst). However, since carbon based support materials are not stable at the high potentials on the anode of a PEM-WE[25,26] and since most oxides have a low electrical conductivity, the choice of possible materials is limited. Antimony doped tin oxide (ATO),[16,27–31] niobium doped titanium oxide (NTO),[32] or tungsten doped titanium oxide (W$_x$Ti$_{1-x}$O$_2$)[33] have been proposed as potential candidates, but there are still concerns whether their long-term stability in the PEM-WE environment and their electrical conductivity is sufficient. In the absence of suitable conductive support material, TiO$_2$ has often been used as a support for Ir based catalysts, since it is stable, commercially available, and inexpensive.[34] However, since TiO$_2$ itself is not conductive, the electrical conductivity needs to be provided by the iridium oxide that is deposited on the TiO$_2$ support. Since a contiguous network/film of Ir or IrO$_2$ nanoparticles is required in order to provide sufficient conductivity across the entire catalyst layer, typically high amounts of Ir or IrO$_2$ are used.[35–37] Unfortunately, this results in catalysts with a high iridium mass fraction which again leads to

relatively high Ir packing densities. This can be illustrated for a commercial OER catalyst that consists of a thick layer of crystalline iridium oxide on a titanium oxide support (c-IrO$_2$/TiO$_2$, with 75 wt% Ir; Elyst Ir75 0480 from Umicore, Germany) and that we had used in previous studies,[6,38] demonstrating that it cannot be used for MEA anode loadings of <0.5 mg$_{Ir}$ cm^{-2} as discussed above. Recently, Regmi et al. developed a catalyst with a thin layer of platinum nanoparticles covering a TiO$_2$ support in order to provide high electrical conductivity without the need of a contiguous network of IrO$_2$.[39] While first results are promising, future studies will have to show whether low Ir electrode loadings (<0.5 mg$_{Ir}$ cm^{-2}) are possible based on this catalyst concept.

In this study, we present a new OER catalyst based on amorphous hydrous iridium oxide supported on titanium oxide (a-IrO(OH)$_x$/TiO$_2$) that was optimized with regards to its Ir packing density by reducing the amount of Ir to only 45 wt% while still maintaining a contiguous iridium oxide film on the support in order to provide sufficient electrical conductivity. The performance of MEAs with low Ir loadings based on the new catalyst in combination with conventional uncoated titanium PTLs (Ti-PTL) or with platinum coated titanium PTLs (Pt-PTL) will be compared to MEAs based on the above described commercial c-IrO$_2$/TiO$_2$ catalyst with 75 wt% Ir. Furthermore, the effect of an additional heat treatment of the new OER catalyst on its activity and conductivity is discussed.

Experimental

Membrane electrode assembly (MEA) preparation and cell assembly.—MEAs with an active area of 5 cm^2 were prepared by using a decal transfer method. The electrodes for the hydrogen evolution reaction on the cathode were prepared from platinum supported on Vulcan XC72 carbon with a metal loading of 45.8 wt % (TEC10V50E, from Tanaka, Japan). For the oxygen evolution reaction on the anode, crystalline c-IrO$_2$/TiO$_2$ (Elyst Ir75 0480 from Umicore, Germany) with 75 wt% Ir or amorphous a-IrO(OH)$_x$/TiO$_2$ with 45 wt% Ir (from Heraeus Deutschland, Germany) were used. The inks were prepared from catalyst powder, 2-propanol (purity $\geqslant$ 99.9%, from Sigma Aldrich), and Nafion® ionomer solution (SGE-10-0ICS, 20 wt% ionomer, D2021 from DuPont, USA). 5 mm ZrO$_2$ grinding beads were added and the ink was mixed for at least 18 h on a roller mill (from Ratek, Australia). The ink was coated onto a 50 μm thick PTFE foil (from Angst+Pfister, Germany) using a Mayer-rod coating machine (Erichsen GmbH & Co. KG, Germany). After drying, electrodes with an active area of 5 cm^2 were punched from the coatings and hot-pressed onto a Nafion® 212 membrane (50 μm, from Quintech, Germany) for 3 min at 155 °C at a pressure of 2.5 MPa. The weight of the electrodes was determined by weighing the PTFE foil decals before and after the decal transfer on a microbalance (±15 μg, from Mettler Toledo, Germany). For the cathodes, the platinum loading was 0.38 ± 0.06 mg$_{Pt}$ cm^{-2}. The iridium loadings on the anodes were 2.33 ± 0.22 mg$_{Ir}$ cm^{-2} for the crystalline c-IrO$_2$/TiO$_2$, with an Ir packing density of $\approx$2.3 g$_{Ir}$ cm^{-3}$_{electrode}$[7] and a resulting anode electrode thickness of $\approx$10 μm, for the amorphous a-IrO(OH)$_x$/TiO$_2$, the loadings were 0.27 ± 0.04 mg$_{Ir}$ cm^{-2}, with an Ir packing density of $\approx$0.5 g$_{Ir}$ cm^{-3}$_{electrode}$ and a resulting anode electrode thickness of $\approx$5 μm.

Carbon fiber paper (TGP-H-120 from Toray, no MPL, 5 wt% PTFE) with a thickness of 370 ± 10 μm was applied as a porous transport layer (PTL) on the cathode side. On the anode, sintered titanium (from Mott Corporation, USA) with a porosity of approximately 50% and a thickness of 280 ± 10 μm was used. Test cells were built either with the untreated titanium PTLs (furtheron referred to as Ti-PTL) or with platinum coated PTLs using the same titanium sinter as a base material (platinum film thickness $\approx$0.5 μm, deposited by Umicore Galvanotechnik, Germany; furtheron referred to as Pt-PTL). The MEA and PTLs were placed between the flow fields of the electrolyzer test cell and sealed with PTFE gaskets (from Reichelt, Germany) with an appropriately

chosen thickness, so that a compression of ≈25% was achieved for the carbon PTL (assuming the titanium PTL to be incompressible; for details see Ref. 38).

Electrochemical characterization.—Tests were performed on a self-built test station equipped with a *BioLogic* VSP 300 potentiostat and a 20 A booster. The measurements were performed at 80 °C cell temperature. Deionized (DI) water was preheated to 80 °C and fed to the anode side of the cell at a rate of 20 ml min^{-1}. Both the anode and the cathode side were kept at ambient pressure. Once the cell was warmed up to 80 °C while feeding water to the anode and dry N$_2$ to the cathode, a conditioning procedure was started, first by ramping up the current to 1 A cm^{-2} and then holding this current for 30 min. Next, galvanostatic polarization curves were recorded at current densities between 0.01 A cm^{-2} and 4 A cm^{-2}. A hold time of 5 min was applied to reach a steady state before recording the cell voltage. At each current setting, AC impedance measurements in a range of 150 kHz − 1 Hz were carried out while applying a current perturbation between ±20 mA– ±500 mA (the current amplitude was chosen for each step to obtain a sufficient signal to noise ratio, while keeping the perturbation small enough to ensure a linear system response). The high-frequency resistance (*HFR*) was determined from the zero crossing of the Nyquist plot with the real axis. Cyclic voltammograms (CVs) of the anode electrode were recorded at the beginning of a test, using a scan rate of 50 mV s^{-1} at 80 °C and a voltage range of 0.1 − 1.3 V. The anode working electrode was flushed with DI water at a rate of 20 ml min^{-1} and the cathode counter electrode was purged with dry H$_2$ at 50 ml min^{-1}.

Heat treatment of the a-IrO(OH)$_x$/TiO$_2$ catalyst.—The heat treatment of the a-IrO(OH)$_x$/TiO$_2$ catalyst was performed by placing ≈2 g of the catalyst in a ceramic vessel which was put into a tube furnace (from *Carbolite Gero*, Germany). Every sample was heat-treated under oxygen atmosphere with the flow rate of oxygen adjusted to 0.8 l min^{-1}. The furnace was heated up at a rate of 10 K min^{-1} until the final temperature, which was chosen between 330 °C–390 °C, was reached. This temperature was held for 3 h before cooling the sample down to room temperature.

Catalyst powder conductivity measurements.—For these measurements, 600–700 mg of the catalyst powder were filled into a homemade sample holder consisting of a plastic cylinder (inner diameter of 6 mm) sitting on a metal plate and being contacted with a metal plunger from the top. This set-up was placed in a mechanical press, so that the catalyst powder could be pressed into a pellet by applying a compressive force of 1040 MPa. The thickness of the compressed pellet could be determined from a scale at the side of the metal plunger (for details, see Ref. 40). The electrical conductivity of the catalyst powder was determined by measuring the voltage response while applying a constant current at the applied pressure of 1040 MPa. For the as-received amorphous a-IrO(OH)$_x$/TiO$_2$ catalyst, currents of 1, 1.5, and 2 mA were chosen, whereas for the crystalline c-IrO$_2$/TiO$_2$ catalyst as well as for the heat-treated a-IrO(OH)$_x$/TiO$_2$ catalysts, currents of 100, 250, and 500 mA were applied; the voltages were recorded after a current hold time of 30 s for each step (note that the currents were selected as to obtain sufficiently high voltage readings). The voltage response was measured with a *BioLogic* VSP 300 potentiostat contacting the metal plunger pressing onto the top of the powder sample as well as the metal plate at the bottom. The electrical conductivity (σ_{el}) of the thus compressed powder can be calculated according to:

$$\sigma_{el} = \frac{t}{A} \cdot \frac{I}{U} \qquad [1]$$

where t is the thickness of the compressed pellet (ranging between ≈1–2 mm), A is the cross-sectional area of the pellet (A = 0.28 cm^2), I is the applied current, and U is the measured voltage response.

Catalyst Design Concept for TiO$_2$ Supported OER Catalysts

In this section, we introduce the general concept proposed for the development of TiO$_2$ supported (hydrous) iridium oxide catalysts that can provide a low Ir packing density; the same considerations also apply to other support materials.

Rationale for the here developed OER catalyst.—The here used commercial catalyst from Umicore consists of mostly crystalline IrO$_2$ on a TiO$_2$ support (c-IrO$_2$/TiO$_2$) with an Ir content of 75 wt%, and is referred to as "Benchmark" catalyst within this study. Assuming that a TiO$_2$ support with a BET surface area of BET$_{TiO_2}$ ≈ 100 m^2 g^{-1} was employed in the synthesis of the Benchmark catalyst (the preferred range is given as BET$_{TiO_2}$ = 100 − 300 m^2 g^{-1} in Ref. 37) and that this support is uniformly covered with IrO$_2$ with a density of ρ_{IrO_2} = 11.7 · 10^6 g m^{-3}, the nominal thickness of a homogenously deposited IrO$_2$ layer (t_{IrO_2}) can be determined from:

$$t_{IrO_2} = \frac{volume_{IrO_2}}{area_{TiO_2}} = \frac{m_{IrO_2}/\rho_{IrO_2}}{m_{TiO_2} \cdot BET_{TiO_2}}$$
$$= \frac{wt\%_{Ir} \cdot (M_{IrO_2}/M_{Ir})}{100\% - wt\%_{Ir} \cdot (M_{IrO_2}/M_{Ir})} \cdot \frac{1}{\rho_{IrO_2} \cdot BET_{TiO_2}} \qquad [2]$$

where m_{IrO2} and m_{TiO2} are the mass of IrO$_2$ and TiO$_2$, respectively, wt%$_{Ir}$ is the iridium mass fraction of the catalyst, and the molar mass of IrO$_2$ and Ir are M_{IrO2} = 224 g mol^{-1} and M$_{Ir}$ = 192 g mol^{-1}. For the Benchmark catalyst, this results in an estimated nominal iridium oxide film thickness of t_{IrO_2} ≈ 6 nm.

An obvious way to reduce the Ir content of an IrO$_2$/TiO$_2$ catalyst without changing the TiO$_2$ support is to reduce the thickness of the IrO$_2$ film. In a series of experiments (data not shown), a nominal film thickness of t_{IrO_2} ≈ 2 nm was found as a lower practical limit that would still yield a sufficiently homogeneous coverage of the TiO$_2$ support, as indicated by the observation that catalysts with t_{IrO_2} values significantly smaller than 2 nm resulted in materials with very poor electrical conductivity (this critical t_{IrO_2} value may, of course, vary for different synthesis processes). A closer inspection of Eq. 2 also shows that the Ir mass fraction for a given targeted t_{IrO_2} value decreases with decreasing BET$_{TiO_2}$ values. In summary, minimizing the nominal t_{IrO_2} value for a given TiO$_2$ support BET and/or reducing the TiO$_2$ support BET for a given nominal t_{IrO_2} value lead to a lowering of the iridium mass fraction of the catalyst (wt%$_{Ir}$) and thus to a decrease of the iridium packing density (shown in more detail below). Hence, for the development of a new OER catalyst with a low iridium packing density (conducted in the framework of the Kopernikus—P2X project[41]), a catalyst was developed by Heraeus Deutschland that consists of an amorphous, hydrous iridium oxide (a-IrO(OH)$_x$) layer deposited on a TiO$_2$ support (a-IrO(OH)$_x$/TiO$_2$), aiming at a nominal t_{IrO_2} value of ≈2 nm (furtheron referred to as "P2X" catalyst within this study).

Table I gives an overview of the properties of the Benchmark and the P2X catalysts. Due to the targeted nominally ≈2 nm thin iridium oxide layer the Ir content of the P2X catalyst was reduced to 45 wt% (consistent with the wt%$_{Ir}$ value that is predicted by a rearrangement of Eq. 2), substantially lower than the 75 wt% for the Benchmark catalyst. As expected, this results in a ≈5-fold lower Ir packing density for the P2X catalyst with only ≈0.5 g$_{Ir}$ cm^{-3}$_{electrode}$ compared to that of the commercial Benchmark catalyst with ≈2.3 g$_{Ir}$ cm^{-3}$_{electrode}$. The Ir packing density was obtained by dividing the catalyst loading (mg$_{Ir}$ cm^{-2}) by the electrode thickness determined from cross-sectional SEM imaging (as explained in Ref. 6).

The OER mass activity (A g$_{Ir}$$^{-1}$) of the catalysts was determined in a single-cell PEM-WE at an iR-corrected cell potential ($E_{iR-free}$ ≡ E_{cell}−i·HFR) of 1.43 V (i.e., at low current densities, where mass transport resistances are usually negligible[38] and the mass activity is not affected by catalyst loading or electrode thickness) at 80 °C and ambient pressure for MEAs with the respective catalyst in combination with a platinum coated PTL (cf Fig. 6). The results given in

Table I. Material properties of the Benchmark catalyst from Umicore and the P2X catalyst from Heraeus Deutschland: i) iridium content (wt%); ii) nominal iridium oxide coating thickness (t_{IrO_2}, see Eq. 2), assuming a uniform coverage of the TiO_2 support by IrO_2 (for the Benchmark catalyst a 100 m^2 g^{-1} BET was assumed); iii) iridium packing density (g$_{Ir}$ cm^{-3}$_{electrode}$) in the catalyst layer. Additionally, the MEA mass activity (A g$_{Ir}$$^{-1}$) determined at an iR-free potential of 1.43 V and the powder conductivity (S cm^{-1}) are given.

	iridium content	nominal IrO_2 coating thickness[a)]	iridium packing density	mass activity at 1.43 $V_{iR-free}$[b)]	powder conductivity
Benchmark (c-IrO_2/TiO_2)	75 wt%	≈6 nm	2.3 g$_{Ir}$ cm^{-3}$_{electrode}$	12 A g$_{Ir}$$^{-1}$	416 S cm^{-1}
P2X a-IrO(OH)$_x$/TiO_2)	45 wt%	≈2 nm	0.5 g$_{Ir}$ cm^{-3}$_{electrode}$	440 A g$_{Ir}$$^{-1}$	0.7 S cm^{-1}

a) based on Eq. 2, assuming a BET area of the TiO_2 support for the Benchmark catalyst of 100 m^2 g^{-1}. b) measured with a platinized titanium PTL (Pt-PTL) at 80 °C and ambient pressure (i.e., $p_{H2} = p_{O2} \approx 53$ kPa$_{abs}$); Ir-loadings were ≈2.33 mg$_{Ir}$ cm^{-2} (Benchmark) and ≈0.27 mg$_{Ir}$ cm^{-2} (P2X).

Table I show a ≈37-fold higher OER mass activity for the P2X catalyst (440 A g$_{Ir}$$^{-1}$) compared to the Benchmark catalyst (12 A g$_{Ir}$$^{-1}$). The majority of this difference can be explained by the roughly one order of magnitude higher intrinsic activity of the amorphous IrO(OH)$_x$ compared to the crystalline IrO_2.[14,15] In addition, a smaller part of this difference can be ascribed to the higher iridium utilization for the P2X catalyst due to the lower nominal iridium oxide film thickness ($t_{IrO_2} \approx 2$ nm) compared to the Benchmark catalyst (estimated to be ≈6 nm), corresponding to an estimated ≈3-fold difference in iridium utilization. However, this advantage in catalytic activity of the a-IrO(OH)$_x$/TiO_2 based P2X catalyst unfortunately comes along with a ≈600-fold lower electrical conductivity (0.7 S cm^{-1}) compared to the c-IrO_2/TiO_2 based Benchmark catalyst (416 S cm^{-1}), as determined by powder conductivity measurements (see Table I, based on. Fig. 4). Again, this is related to the nature of the iridium oxide, since a-IrO(OH)$_x$ is known to have a lower conductivity compared to c-IrO_2[23,24]: in addition, the lower nominal IrO_2 film thickness of the P2X catalyst renders it more likely that not all of the electrically insulating TiO_2 is covered by the a-IrO(OH)$_x$ species that are poorly conducting, but not insulating. A detailed analysis of the nature of the iridium oxide species and the coverage of the TiO_2 support material will be published in a separate study.[42]

With its ≈5-fold lower Ir packing density (≈0.5 g$_{Ir}$ cm^{-3}$_{electrode}$) compared to the Benchmark catalyst (≈2.3 g$_{Ir}$ cm^{-3}$_{electrode}$), the P2X catalyst allows for a lower Ir loading at a similar electrode thickness. In a previous study, we found an electrode thickness of $t_{electrode}$ ≈5 μm to be the lower limit until which no negative effect on the PEM-WE performance was observed, while thinner electrodes resulted in a deterioration of the high current density performance.[6] At the measured Ir packing density of $\rho_{Ir-packing} \approx 0.5$ g$_{Ir}$ cm^{-3}$_{electrode}$, this translates into an Ir loading of only $L_{Ir} \approx 0.25$ mg$_{Ir}$ cm^{-2} (from $L_{Ir} = t_{electrode} \cdot \rho_{Ir-packing}$), which is a ≈8-fold reduction compared to a typical loading of ≈2 mg$_{Ir}$ cm^{-2} for state-of-the-art commercial PEM-WEs.[1,4,5] Despite this significant advance, the projected minimum iridium loading is still 5 times higher compared to the ≈0.05 mg$_{Ir}$ cm^{-2} target required in order to allow for PEM-WE installation capacities of ≥100 GW year^{-1} that would be required for a global H$_2$ economy based on H$_2$ produced by PEM-WE.[6,7]

Future design strategies for OER catalysts with low iridium packing densities.—Since the nominal thickness of the iridium oxide layer cannot be reduced below ≈2 nm without sacrificing the contiguous iridium oxide network that is required to provide a sufficiently high electrical conductivity across/within the catalyst layer, another way to reduce the iridium packing density in the electrode based on an IrO_2/TiO_2 OER catalyst concept is to use a TiO_2 support with a lower specific surface area. This is illustrated in the following, based on several simplifying assumptions: i) the packing density of a lower specific surface area TiO_2 support ($\rho_{TiO_2-packing}$) remains the same as that for the commercial TiO_2 support used in this section; ii) the molecular mass of the iridium oxide species which would be deposited on the TiO_2 support is reasonably close to that of IrO_2 (in the most extreme case, for Ir(OH)$_4$-like species, the difference

is ≈16%); and, iii) the size of the TiO_2 support is significantly less than the targeted thickness of the electrode.

First, we determine the TiO_2 support packing density ($\rho_{TiO_2-packing}$) for a commercially available TiO_2 support (Aeroxide® P25, from Sigma Aldrich) with a BET surface area in the range of 35–65 m^2 g^{-1} (for the calculations made in this section an average surface area of BET$_{TiO_2} \approx 50$ m^2 g^{-1} is assumed). For this purpose, electrodes were fabricated with the TiO_2 similar to the electrodes with the actual catalyst materials and hot-pressed onto a Nafion® 212 membrane as described in the experimental section. The TiO_2 packing density can be obtained by dividing the TiO_2 loading (mg$_{TiO2}$ cm^{-2}) by the electrode thickness determined from cross-sectional SEM imaging (as explained in Ref. 6).

For the commercial TiO_2 support a packing density of $\rho_{TiO_2-packing} \approx 1.18$ g$_{TiO_2}$ cm^{-3}$_{electrode}$ was obtained, which corresponds to a TiO_2 volume fraction in the electrode of $\varepsilon_{TiO_2} \approx 0.28$ (from $\rho_{TiO_2-packing}/\rho_{TiO_2}$). This is much lower than the expected volume fraction for closest packing of spheres ($\varepsilon_{CP} \approx 0.74$), but higher than that of the high-structure carbon blacks used for PEM fuel cells ($\varepsilon_{C-black} \approx 0.16$[43]). In general, the volume fraction of the support material depends on the shape of the TiO_2 particles and, consequently, even lower volume fractions might be possible for differently shaped TiO_2 particles. Based on a spherical approximation assuming solid TiO_2 spheres with a density of $\rho_{TiO_2} = 4.23 \cdot 10^6$ g m^{-3} for the 50 m^2 g^{-1} TiO_2 support, the average radius of the TiO_2 particles is $r_{TiO2} \approx 14$ nm ($r_{TiO2} \approx 3/(\rho_{TiO_2} \cdot BET_{TiO_2})$), which is large compared to the nominal iridium oxide film thickness of $t_{IrO_2} \approx 2$ nm. Therefore, the packing density of the final catalyst consisting of the TiO_2 support with a ≈2 nm thick iridium oxide film on its surface should not be significantly affected by the deposited iridium species.

In the following, we will assume that TiO_2 supports with lower specific surface area can also be obtained at comparable TiO_2 packing densities ($\rho_{TiO_2-packing} \approx 1.18$ g$_{TiO_2}$ cm^{-3}$_{electrode}$), resulting in electrodes with a comparable TiO_2 volume fraction ($\varepsilon_{TiO_2} \approx 0.28$). For a targeted electrode thickness of $t_{electrode} = 5$ μm (found to be the ideal thickness for a PEM-WE anode[6]), the corresponding TiO_2 loading (L_{TiO_2}) would then amount to:

$$L_{TiO_2} = \rho_{TiO_2-packing} \cdot t_{electrode} \qquad [3]$$

Using the above TiO_2 packing density, this equates to a projected TiO_2 loading of $L_{TiO_2} \approx 0.59$ mg$_{TiO_2}$ cm^{-2}. If this conceptual TiO_2 support is coated with a nominally homogeneous IrO_2 layer of thickness t_{IrO_2} (assuming $t_{IrO2} \ll r_{TiO2}$), the resulting iridium loading of the electrode can be calculated as:

$$L_{Ir} = L_{TiO_2} \cdot BET_{TiO_2} \cdot t_{IrO_2} \cdot \rho_{IrO_2} \cdot \frac{M_{Ir}}{M_{IrO_2}} \qquad [4]$$

For a TiO_2 support BET area of BET$_{TiO_2} \approx 50$ m^2 g^{-1} and an IrO_2 film thickness of $t_{IrO_2} \approx 2$ nm, the predicted IrO_2 loading of a 5 μm thick electrode would be $L_{Ir} \approx 0.56$ mg$_{Ir}$ cm^{-2}.

The relationship between the iridium electrode loading and the TiO$_2$ BET area for a 5 μm thick electrode is shown in Fig. 1 for a nominal IrO$_2$ film thickness of $t_{IrO_2} \approx 2$ nm (red line, right-hand y-axis). This illustrates that for a $\approx$5 m^2 g^{-1} TiO$_2$ support, an Ir loading of $\approx$0.06 mg$_{Ir}$ cm^{-2} (red line in Fig. 1) can be realized for a 5 μm thick electrode, fulfilling the target for Ir loading reduction defined before. Based on a rearrangement of Eq. 2, the iridium content of a catalyst based on a $\approx$5 m^2 g^{-1} TiO$_2$ support and a nominal IrO$_2$ film thickness of $t_{IrO_2} \approx 2$ nm would amount to $\approx$9 wt %. Even if a slightly thicker iridium oxide layer of $t_{IrO_2} \approx 4$ nm would be required (e.g., to provide better electrical conductivity), an Ir loading of $\approx$0.11 mg$_{Ir}$ cm^{-2} at an electrode thickness of 5 μm would be possible (the resulting iridium content would then be $\approx$16 wt%, based on Eq. 2) based on a $\approx$5 m^2 g^{-1} TiO$_2$ support (purple line in Fig. 1). In general, reducing the surface area of the TiO$_2$ support means increasing the size of the TiO$_2$ primary particles that form the support. For the simplest assumption of spherical TiO$_2$ primary particles, a reduction of the TiO$_2$ surface area from $\approx$50 m^2 g^{-1} to $\approx$5 m^2 g^{-1} would result in an increase of the TiO$_2$ primary particle radius from $r_{TiO2} \approx 14$ nm to $r_{TiO2} \approx 142$ nm (see above), as illustrated by the two sketches in Fig. 1. The approximate TiO$_2$ primary particle radius of $\approx$142 nm still satisfies the above-mentioned requirement that it must be substantially smaller than the targeted electrode thickness. This illustrates how a low surface area TiO$_2$ support in combination with a nominal iridium oxide layer thickness between $\approx$2–4 nm could provide an OER catalyst with an extremely low Ir packing density that would enable ultra-low iridium loadings for sufficiently thick electrodes ($\approx$5 μm).

Of course, reducing the TiO$_2$ surface area and, hence, the iridium loading while keeping the electrode thickness fixed at 5 μm will also result in a lower IrO$_2$ roughness factor, i.e., in a lower ratio of the active IrO$_2$ surface area to the geometric area of the electrode (in units of cm$^2_{IrO2}$ cm$^{-2}_{electrode}$). As long as the nominal thickness of the IrO$_2$ film is small compared to the radius of the TiO$_2$ primary particles, the IrO$_2$ roughness factor (rf_{IrO2}) is approximately the same as that of the TiO$_2$ support:

$$rf_{\mathbf{IrO2}} \approx rf_{\mathbf{TiO2}} = L_{\mathbf{TiO2}} \cdot \mathbf{BET_{TiO2}} \qquad [5]$$

The resulting relationship is shown as dashed black line in Fig. 1 (left-hand y-axis) vs the BET area of the TiO$_2$ support. For a reduction of the TiO$_2$ surface area from $\approx$50 m^2 g^{-1} for the commercial TiO$_2$ support to, for example, $\approx$5 m^2 g^{-1}, the IrO$_2$ roughness factor will be reduced by $\approx$10-fold. However, taking the typical OER Tafel slope of an iridium based catalyst (45–50 mV dec^{-1}),[6,38] this will result in a voltage increase of only 45–50 mV, which seems to be a relatively small penalty considering the significant potential for Ir loading reduction (for a more detailed discussion, see Ref. 7). In the following section, the MEA performance of the P2X catalyst (2 nm iridium oxide film on TiO$_2$ support) will be compared to the commercial Benchmark catalyst.

Results

MEA performance for different catalysts and PTLs.—The MEAs based on the Benchmark catalyst (c-IrO$_2$/TiO$_2$ with 75 wt% Ir from Umicore) have an Ir loading of $\approx$2.33 mg$_{Ir}$ cm^{-2}, which translates into an electrode thickness of $\approx$10 μm (packing density: $\approx$2.3 g$_{Ir}$ cm^{-3}) and can be considered a typical loading for state-of-the-art commercial PEM-WEs.[1,4,5] On the other hand, for the MEAs based on the P2X catalyst (a-IrO(OH)$_x$/TiO$_2$ with 45 wt% Ir from Heraeus Deutschland), the goal was to reduce the Ir loading as far as possible without sacrificing MEA performance that was observed to decrease for catalyst layers much thinner than $\approx$5 μm.[6] Consequently, an electrode thickness of $\approx$5 μm was aimed for when using the P2X catalyst. At the finally obtained Ir loading of $\approx$0.27 mg$_{Ir}$ cm^{-2}, the electrode thickness was $\approx$5.4 μm, corresponding to a packing density $\approx$0.5 g$_{Ir}$ cm^{-3}. The Pt loading on the cathode was $\approx$0.38 mg$_{Pt}$ cm^{-2} for all MEAs.
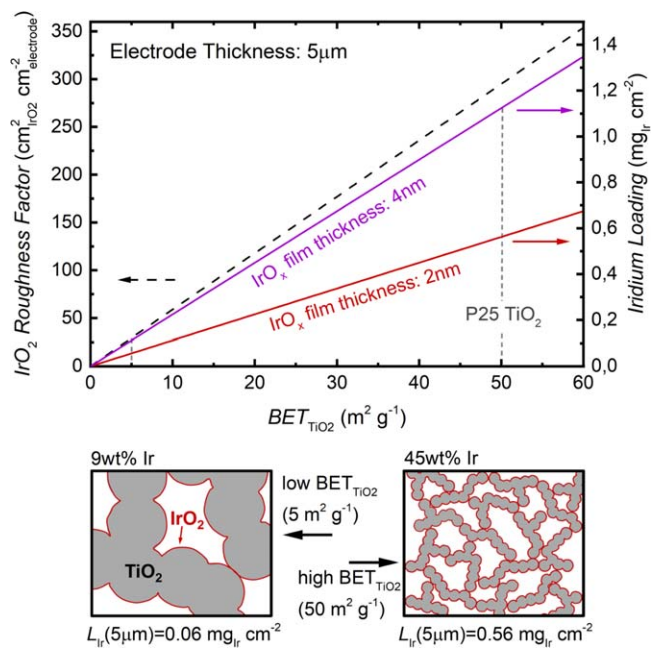

Figure 1. Upper Panel: projected iridium loading of a 5 μm electrode (right-hand y-axis) as a function of the BET surface area of the TiO$_2$ support (BET$_{TiO2}$) for a nominal iridium oxide film thickness of $t_{IrO_2} \approx 2$ nm (red line) and $t_{IrO_2} \approx 4$ nm (purple line), based on Eq. 4 with an estimated TiO$_2$ packing density of $\rho_{TiO2} \approx 1.18$ g$_{TiO2}$ cm$^{-3}_{electrode}$ (see text). The black dashed line shows the IrO$_2$ roughness factor (left-hand y-axis), i.e., ratio of actual IrO$_2$ surface area to the geometric area of the electrode (in units of cm$^2_{IrO2}$ cm$^{-2}_{electrode}$) vs BET$_{TiO2}$ at a fixed electrode thickness of 5 μm (based on Eq. 5). Sketches in the lower panel: These illustrate the structure of the catalyst layer for a TiO$_2$ support with a BET surface area of 50 m^2 g^{-1} (right-hand side), corresponding to an average TiO$_2$ primary particle radius of $\approx$14 nm (see text) as well as with 5 m^2 g^{-1} (left-hand side), corresponding to an average primary TiO$_2$ primary particle radius of $\approx$142 nm (see text). The projected iridium loading (L_{Ir}) at an electrode thickness of 5 μm as well as the Ir content of the catalyst are also given.

Figure 2a shows polarization curves for these two types of MEAs with an untreated titanium PTL (Ti-PTL) as well as with a platinized titanium PTL (Pt-PTL) on the anode, recorded in a 5 cm^2 single-cell PEM-WE at 80 °C and ambient pressure (i.e., at H$_2$ and O$_2$ partial pressures of $\approx$53 kPa). For the MEAs based on the Benchmark catalyst (blue curves in Fig. 2a), the polarization curves are similar, with a slightly lower cell voltage at high current densities ($\Delta E \approx$ 26 mV at 3 A cm^{-2}) for the platinized PTL (light blue dashed line with open circles) compared to the untreated Ti-PTL (dark blue full line and full circles). This can be explained by the $\approx$6.2 mΩcm^2 lower high frequency resistance (HFR) for the platinized PTL (46.9 ± 0.5 mΩcm^2) compared to the Ti-PTL (53.1 ± 0.5 mΩcm^2) as shown in Fig. 2b. Since the membrane resistance should be identical for both MEAs, the lower HFR for the platinized PTL suggests a lower contact resistance between the anode catalyst layer and the PTL for the Pt-PTL compared to the Ti-PTL. The difference in HFR results in a difference in the ohmic overpotential of $\approx$19 mV at 3 A cm^{-2} and, hence, almost completely explains the potential difference between the polarization curves at 3 A cm^{-2} ($\Delta E \approx 26$ mV). Consequently, the iR-free cell voltage (not shown) is similar for both tests with a difference of less than 10 mV, which is expected since the Pt coating of the PTL should only have an influence on the electrode/PTL contact resistance but not on any other voltage losses.

For the MEA based on the P2X catalyst in combination with a Pt-PTL (light red dashed line and open squares in Fig. 2a), the cell voltage is even lower than for the MEAs with the Benchmark catalyst ($\approx$50 mV at 3 A cm^{-2}) despite of the much lower Ir loading of $\approx$0.27 mg$_{Ir}$ cm^{-2} vs $\approx$2.33 mg$_{Ir}$ cm^{-2} for the Benchmark
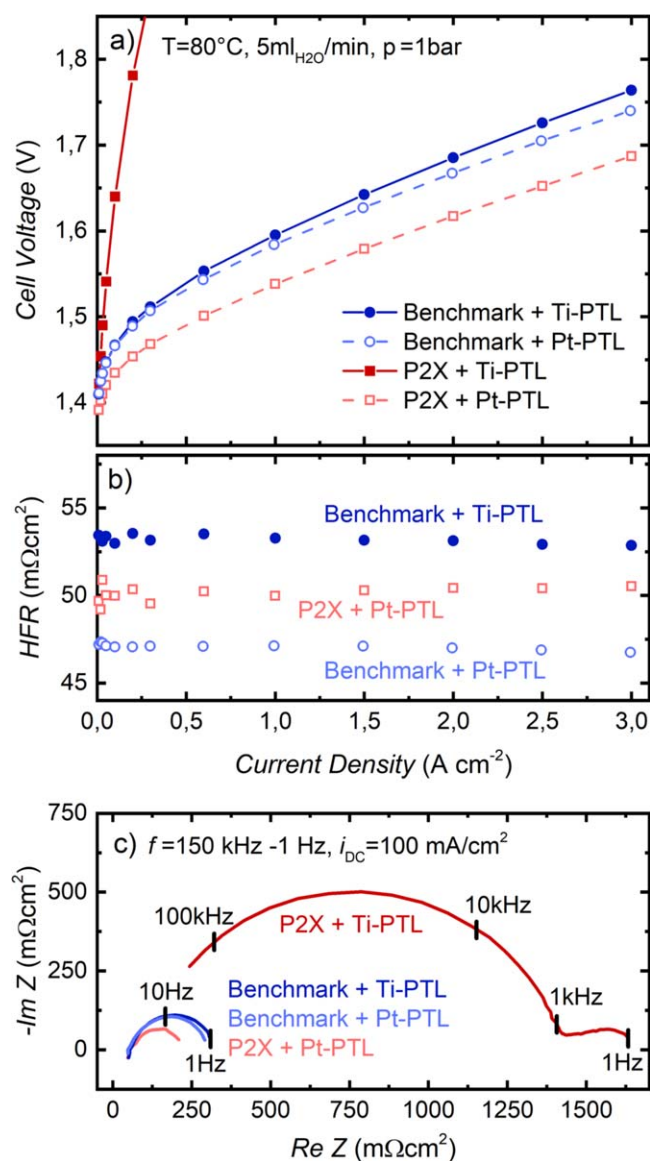
Figure 2. (a) Ambient pressure polarization curves at 80 °C measured for a 5 cm² single-cell PEM-WE with MEAs with a Nafion® 212 membrane and a cathode catalyst loading of ≈0.38 mg$_{Pt}$ cm^{-2} at an anode water feed rate of 20 ml$_{H_2O}$ min^{-1}. On the anode, either the Benchmark catalyst from Umicore (blue) at a loading of ≈2.33 mg$_{Ir}$ cm^{-2} or the P2X catalyst from Heraeus Deutschland (red) at a loading of ≈0.27 mg$_{Ir}$ cm^{-2} were used. Full symbols along with full lines show the data measured with a platinized PTL (Pt-PTL), while open symbols along with dashed lines represent measurements with the untreated titanium PTL (Ti-PTL). (b) Corresponding *HFR*-values vs current density obtained by electrochemical impedance spectroscopy. (c) Nyquist plot of impedance measurements at a constant current density of i_{DC} = 0.1 A cm^{-2} for the Benchmark catalyst in combination with either a Ti-PTL (dark blue) or a Pt-PTL (light blue), or for the P2X catalyst in combination with either a Ti-PTL (dark red) or a Pt-PTL (light red). The impedance data were recorded with a current perturbation of i_{AC} = 0.012 A cm^{-2} in a frequency range of f = 150 kHz–1 Hz. Key frequencies are marked by black lines for the P2X catalyst and the Benchmark catalyst both in combination with a Ti-PTL.

catalyst. Since the *HFR* is even slightly higher compared to that of the MEAs based on the Benchmark catalyst (50.1 ± 0.9 mΩcm² vs 46.9 ± 0.5 mΩcm²), this can be explained by a lower overpotential for the OER due to the much higher mass activity of the catalyst (see values listed in Table I; cf Fig. 6 for a detailed analysis of the OER kinetics). On the other hand, if an MEA with the P2X catalyst is combined with an untreated Ti-PTL, the MEA performance is very

poor, with a cell voltage of >1.8 V at a current density of only 0.25 A cm^{-2} (cf dark red full line and full squares in Fig. 2a). This significantly lower performance can be explained by analyzing the electrochemical impedance spectra, which were recorded at each step of the polarization curve.

Figure 2c exemplarily shows the Nyquist plot of the impedance spectra recorded at a DC current density of i_{DC} = 0.1 A cm^{-2}. In general, the impedance spectra at this current density are expected to consist mainly of a large semicircle which can be attributed to the OER. Indeed, for the MEAs based on the Benchmark catalyst, only one semicircle with a diameter of ≈200 − 250 mΩcm² is visible for both platinized and untreated PTLs (blue lines in Fig. 2c). To a first approximation, the diameter of the semicircle corresponds to the charge transfer resistance of the OER and should be proportional to $1/i_{DC}$; the charge transfer resistance of the hydrogen evolution reaction (HER) for a Pt loading of 0.38 mg$_{Pt}$ cm^{-2} is expected to amount to only ≈1 mΩcm² and, hence, can be neglected (cf Ref. 6 for detailed calculation of HER charge transfer resistances). For a detailed investigation of the impedance spectra, the proton transport resistance in the electrodes and mass transport effects would have to be analyzed as well, which, however, was not the goal of this study.

The impedance spectrum of the MEA based on the P2X catalyst in combination with the platinized PTL (light red line in Fig. 2c) shows a similar shape compared to the Benchmark catalyst, with a slightly smaller semicircle diameter of ≈150 mΩcm², indicating a lower OER charge transfer resistance. For the MEA with the P2X catalyst in combination with the untreated Ti-PTL (dark red line in Fig. 2c), the impedance spectrum is completely different, showing two semicircles. The semicircle at lower frequencies (the one at the right-hand-side) has a similar size compared to the one observed for the platinized PTL (light red line in Fig. 1c) and is recorded in the same range of frequencies (≈1 kHz—1 Hz), hence, representing the OER kinetics. On the other hand, the large semicircle observed at high frequencies (>1 kHz, i.e., the one on the left-hand-side) can be attributed to an electrical contact resistance (which can be described by a RC-element). As the high frequency semicircle still does not approach the x-axis in the Nyquist plot at the maximum frequency of 150 kHz (cf Fig. 2c; higher frequencies cannot be evaluated with sufficient accuracy with the current setup), the *HFR* can only be estimated by extrapolation (ranging in between ≈50–150 mΩcm²) and thus is rather imprecise. The assignment of the high frequency semicircle to a contact resistance is based on previous observations and assignments for the behavior of electrodes in lithium-ion batteries.[44] For example, Landesfeind et al. detected a similar semicircle at high frequencies for a lithium iron phosphate based electrode that has a poor electrical conductivity, showing that the diameter of the semicircle depends on the compressive force applied on the electrode and, hence, can be attributed to a contact resistance between electrode and metal substrate.[45] Since the high frequency semicircle can be observed only for the P2X catalyst in combination with the untreated Ti-PTL, while at the same time it disappears completely when a platinized PTL is used, it can clearly be attributed to a contact resistance at the interface between catalyst layer and the PTL. The value of this contact resistance can be estimated by the diameter of the high frequency semicircle to ≈1 Ωcm². This is ≈100 times higher than the electric contact resistance determined for the Benchmark catalyst in combination with a Ti-PTL (≈10 mΩcm²) in a previous study.[38] The semicircle for such a low contact resistance (≈10 mΩcm²) would appear in a ≈100 times higher frequency range (i.e., at frequencies >100 kHz) and, hence, cannot be observed in the recorded impedance spectra for the P2X catalyst in combination with the Pt-PTL as well as for the Benchmark catalyst. In this case, the *HFR* is generally considered to represent the sum of membrane resistance and electric contact resistances.

The origin of the high electrical contact resistance for the P2X catalyst in combination with the Ti-PTL can be found in the combination of a catalyst layer with a relatively low conductivity (a-IrO(OH)$_x$/TiO$_2$) and the untreated Ti-PTL which passivates at the conditions on the anode of a PEM-WE, i.e., which forms a thin non-
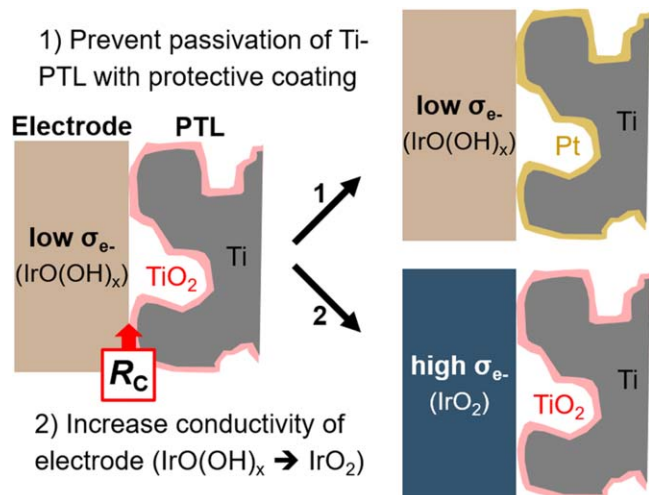
Figure 3. Sketch illustrating the combination of material properties that is required to prevent the formation of an electrical contact resistance at the interface between the catalyst layer and the PTL. The passivation of an untreated Ti-PTL in combination with a catalyst layer with a low electric conductivity (e.g., the a-IrO(OH)$_x$/TiO$_2$ based P2X catalyst) leads to the formation of an electrical contact resistance (sketch on the left). This contact resistance can be avoided by: 1) preventing the passivation of the Ti-PTL by applying a protective platinum coating (upper right-hand-side sketch) or by 2) using a highly conductive catalyst material like, e.g., the c-IrO$_2$/TiO$_2$ based Benchmark catalyst (lower right-hand-side sketch).

Figure 4. Catalyst powder conductivity measured at a compressive force of 1040 MPa for the untreated P2X catalyst (a-IrO(OH)$_x$/TiO$_2$) from Heraeus Deutschland(red triangle), the Benchmark catalyst (c-IrO$_2$/TiO$_2$) from Umicore (blue circle), as well as for the P2X catalyst after heat treatment in pure O$_2$ atmosphere for 3 h at temperatures from 330 °C–390 °C (green triangles).

conductive layer of TiO$_2$ on its surface as illustrated on the left side of Fig. 3. Only the combination of these two factors (a low catalyst layer conductivity + a poorly conducting PTL surface) leads to the formation of a large electrical contact resistance and the resulting poor MEA performance observed in Fig. 2a. If a highly conductive catalyst is used (c-IrO$_2$/TiO$_2$, Benchmark), the electrical contact resistance will remain low, even in combination with an untreated Ti-PTL (cf bottom right part of Fig. 3); the difference in the electrical contact resistance between the c-IrO$_2$/TiO$_2$ based catalyst layer and either a Pt-PTL or a Ti-PTL is shown to be only ≈6 mΩcm^2 (cf Fig. 2b). This effect of the catalyst layer conductivity on the electrode/ PTL contact resistance could already be shown in a previous study, where the combination of the c-IrO$_2$/TiO$_2$ Benchmark catalyst with a Ti-PTL also resulted in a low electrode/PTL contact resistance.[46] However, when the crystalline IrO$_2$ was transformed into an amorphous IrO(OH)$_x$ with a lower electrical conductivity during an accelerated stress test, the electrical contact resistance increased by ≈30 mΩcm^2.[46] A possibility to reduce this contact resistance even for catalyst layers with a relatively low electrical conductivity (e.g., a-IrO(OH)$_x$/TiO$_2$) is to prevent the passivation of the Ti-PTL by applying a protective coating (cf top right sketch in Fig. 3). Typically, platinum is used to coat PTLs which adds significant cost to the PEM-WE stack.[4] Other potential coating materials (especially non-noble metal materials) are being investigated in order to minimize costs, but of course the best option would be to entirely eliminate the need for a coating. Since this is possible for catalyst layers with a high electrical conductivity, we will investigate in the following section the effect of a heat treatment on the electrical conductivity of the a-IrO(OH)$_x$/TiO$_2$ P2X catalyst.

Heat treatment of the a-IrO(OH)$_x$/TiO$_2$ based P2X catalyst.—In order to increase the electrical conductivity of the a-IrO(OH)$_x$/TiO$_2$ catalyst, a heat treatment at temperatures from 330 °C–390 °C in O$_2$ atmosphere was applied as described in the experimental section. It is well known that calcination at elevated temperatures leads to a transformation of amorphous IrO(OH)$_x$ to crystalline IrO$_2$,[14] which has a lower catalytic activity but a higher electrical conductivity.[23,24] In order to evaluate the electrical conductivity of the catalyst after
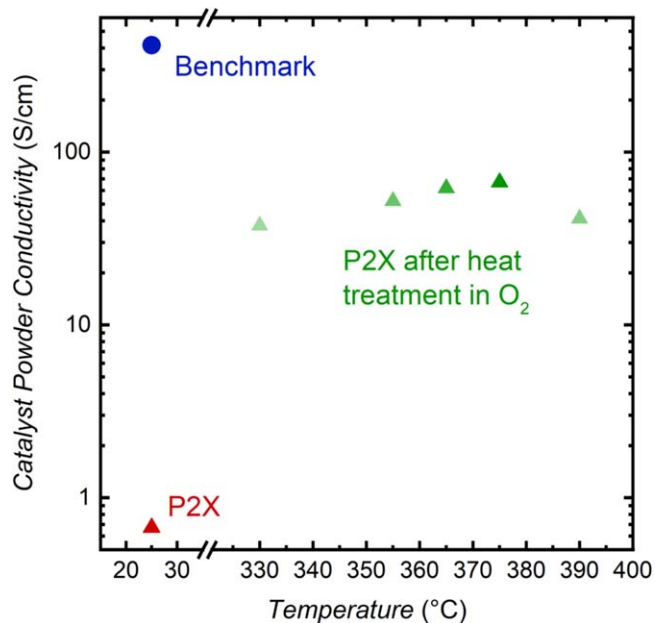
calcination, powder conductivity measurements were performed (cf Fig. 4).

The untreated P2X catalyst (a-IrO(OH)$_x$/TiO$_2$) has a powder conductivity of 0.7 S cm^{-1} (red triangle in Fig. 4), which is nearly three orders of magnitude lower compared to that of the Benchmark catalyst (c-IrO$_2$/TiO$_2$) with a conductivity of 416 S cm^{-1} (blue circle in Fig. 4). Upon the heat treatment, the conductivity of the P2X catalyst increases substantially (green triangles in Fig. 4) to 38 S cm^{-1} at 330 °C up to a maximum of 67 S cm^{-1} at 375 °C, while it drops back to 41 S cm^{-1} for a heat treatment temperature of 390 °C. The increase of conductivity at higher temperatures can be explained with an increasing degree of crystallization of the initially amorphous IrO(OH)$_x$. However, higher heat treatment temperatures are also expected to lead to significant sintering of the iridium oxide nanoparticles (e.g., for hydrous iridium oxide supported on antimony doped tin oxide, substantial sintering was observed above 350 °C[47]), and the formation of larger IrO$_2$ nanoparticles would have to result in a disruption of the initially more continuous iridium oxide network that provides electrical conductivity throughout the catalyst layer, a phenomenon that could explain the lower electrical conductivity for temperatures above 375 °C. This effect is described in more detail in a study by other partners in this project that also investigates the effect of a heat treatment procedure on the conductivity of the P2X catalyst.[42] Even though a different heat treatment procedure was used there, the same optimum in conductivity for a calcination temperature of 375 °C was found.

The catalyst that was heat-treated at 375 °C (i.e., the material with the highest conductivity among the heat-treated P2X catalysts) was used to fabricate MEAs, which in the following will be compared to MEAs with the Benchmark catalyst and the untreated P2X catalyst. Cyclic voltammograms (CVs) of the catalysts incorporated into MEAs were recorded at the beginning of single-cell PEM-WE tests in order to obtain insights into the surface chemistry of the Ir-based anode catalysts (cf Fig. 5). The CV of the Benchmark catalyst (c-IrO$_2$/TiO$_2$) does not show well-defined redox features, which is characteristic of crystalline IrO$_2$[15] (blue line in Fig. 5). On the other hand, the untreated P2X catalyst (a-IrO(OH)$_x$/TiO$_2$) shows
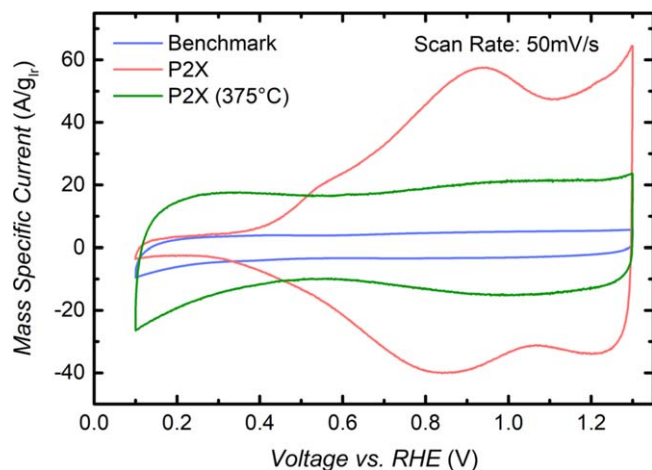
Figure 5. Ambient pressure cyclic voltammograms (CV) of the P2X catalyst from Heraeus Deutschland (red), the Benchmark catalyst from Umicore (blue), as well as the P2X catalyst after heat treatment at 375 °C (green). The mass-specific current is plotted vs the applied potential. CVs were recorded with 5 cm² active area MEAs at a scan rate of 50 mV s⁻¹ at 80 °C. H_2O was supplied to the anode at 5 ml_{H2O} min⁻¹, and dry H_2 was supplied to the cathode at 50 ml min⁻¹ (the Ir-based anodes served as working electrodes, and the Pt-based cathodes as counter and reference electrode).
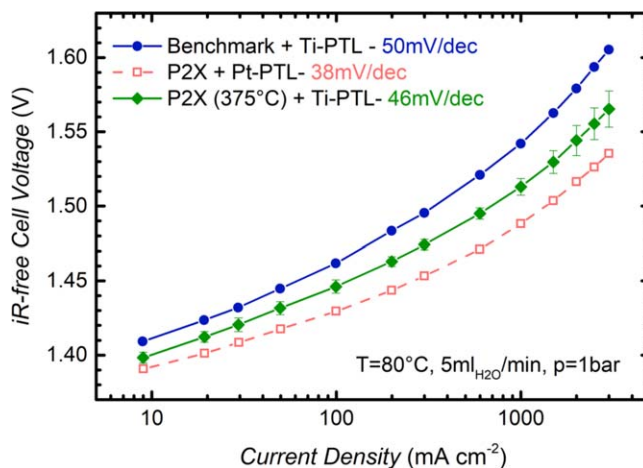

Figure 6. Ambient pressure Tafel plot of the iR-free cell voltage of a 5 cm² single-cell PEM-WE for MEAs with a Nafion® 212 membrane and a cathode catalyst loading of ≈0.38 mg_{Pt} cm⁻² at a temperature of 80 °C. The blue curve represents the Benchmark catalyst from Umicore at a loading of ≈2.33 mg_{Ir} cm⁻² in combination with an untreated Ti-PTL. The red curve shows the untreated P2X catalyst from Heraeus Deutschland in combination with a platinized PTL (Pt-PTL), while the green curve presents the average of three MEAs using the P2X catalyst heat-treated in O_2 at 375 °C in combination with a Ti-PTL (anode catalyst loadings: ≈0.27 mg_{Ir} cm⁻²). The Tafel slope is obtained from a linear fit of the values between 10–100 mA cm⁻².

redox features that can be attributed to the transition between Ir(III)/Ir(IV) along with a much higher mass specific current at potentials >0.7 V, which is characteristic for a hydrous a-IrO(OH)$_x$[15] (red line in Fig. 5). After the heat-treatment at 375 °C, these redox peaks disappear and the shape of the CV is similar to the one of the Benchmark catalyst, i.e., resembling that of mainly crystalline IrO_2 (green line in Fig. 5). This strongly indicates the transition of the amorphous IrO(OH)$_x$ to a crystalline IrO_2 due to the heat-treatment as discussed before.

While the shape of the CV of the P2X catalyst heated to 375 °C (referred to as P2X (375 °C)) is similar to the one of the Benchmark catalyst (blue line), the mass specific capacitive currents are ≈3 − 4 times higher for the P2X (375 °C) catalyst (green line). Assuming a similar surface chemistry, this would translate directly into a ≈3 − 4 times higher electrochemical surface area (ECSA) normalized to the Ir-loading (m² g_{Ir}⁻¹) for the P2X (375 °C) catalyst compared to the Benchmark catalyst. This significant difference, we believe, can largely be attributed to the different nominal IrO_2 film thickness on the TiO_2 support of the P2X catalyst (≈2 nm) compared to the Benchmark catalyst (≈6 nm) that was estimated in the previous section (see Table I). For the thick IrO_2 layer of the Benchmark catalyst, a relatively high amount of the Ir atoms is located in the bulk of the IrO_2 phase and, consequently, not electrochemically accessible, while for the rather thin IrO_2 layer of the P2X catalyst, more Ir atoms are at the surface and thus lead to a higher catalyst utilization.

These differences in the catalyst structure and the nature of the iridium oxide have a significant impact on the OER activity of the catalysts. Figure 6 shows the *HFR*-corrected cell voltage ($E_{iR-free} = E_{cell}-i·HFR$) of a 5 cm² active area single-cell PEM-WE for the different MEAs plotted vs the logarithm of the current density (i.e., as a Tafel plot). The Tafel slopes are obtained from a fit of the linear region between 10–100 mA cm⁻², where voltage losses due to proton transport or mass transport are negligible,[38] so that the iR-free cell voltage directly represents the OER kinetics. The Benchmark catalyst has a Tafel slope of 50 mV dec⁻¹ (blue curve in Fig. 6), which is in agreement with the values of 45–50 mV dec⁻¹ found in our previous studies for the same catalyst.[6,38] The untreated P2X catalyst that has not undergone a heat treatment (red curve in Fig. 6) has a Tafel slope of only 38 mV dec⁻¹, indicating a different reaction mechanism for the a-IrO(OH)$_x$ compared to the c-IrO$_2$ of

the Benchmark catalyst. Additionally, the mass activity of the P2X catalyst—determined at an iR-free cell voltage of 1.43 V—is much higher with 440 A g_{Ir}⁻¹ compared to the Benchmark catalyst with only 12 A g_{Ir}⁻¹ (see also Table I). There are two factors which can explain this difference: i) a higher mass activity of the amorphous IrO(OH)$_x$ compared to the crystalline IrO_2[14,15]; and, ii) a higher utilization of the iridium oxide for the P2X catalyst due to the much lower film thickness (≈2 nm) compared to the Benchmark catalyst (estimated to be ≈6 nm, see Table I). After the heat treatment of the a-IrO(OH)$_x$/TiO$_2$ based P2X catalyst at 375 °C, the Tafel slope of the P2X catalyst increases to 46 mV dec⁻¹ and the mass activity drops to 167 A g_{Ir}⁻¹ (green curve in Fig. 6). Again, this can be explained by the transformation of the amorphous IrO(OH)$_x$ to crystalline IrO_2, which is known to have a lower OER activity.[14,15] A similar change in the OER Tafel slope (measured in 0.5 M H_2SO_4) was observed by Karimi et al.[47] upon heat treatment in air for hydrous iridium oxide deposited on antimony doped tine oxide (ATO), showing a gradual increase from ≈40 mV dec⁻¹ for the pristine material to ≈46 mV dec⁻¹ for a the material heated to ≈380 °C, all the way to ≈57 mV dec⁻¹ for a material heated to ≈700 °C, where crystalline IrO_2 had been formed; at the same time, the mass activity decreased substantially with heat treatment temperature, consistent with references[14] and.[15] Overall, while the OER mass activity of the P2X (375°C) catalyst decreased compared to the untreated P2X catalyst, its OER mass activity is still ≈14 times higher compared to the Benchmark catalyst, more than one would expect simply based on the higher ECSA determined from the CVs (factor of ≈3–4, cf Fig. 5). Additionally, the Tafel slope is still slightly lower compared to the Benchmark catalyst. Both findings suggest that the heat treatment at 375 °C did not lead to a complete transformation of the amorphous IrO(OH)$_x$ into crystalline IrO_2 and that there are still amorphous IrO(OH)$_x$ species present. This is also supported by X-ray diffraction data and Raman spectroscopy results published in a separate study.[42]

In summary, the heat treatment of the P2X catalyst in O_2 at 375 °C led to a partial transformation of the initially amorphous IrO(OH)$_x$ into crystalline IrO_2, resulting in a ≈100-fold increase of the electrical conductivity, while the OER mass activity decreased by only ≈2.5-fold. Nevertheless, the mass activity of the P2X (375 °C)
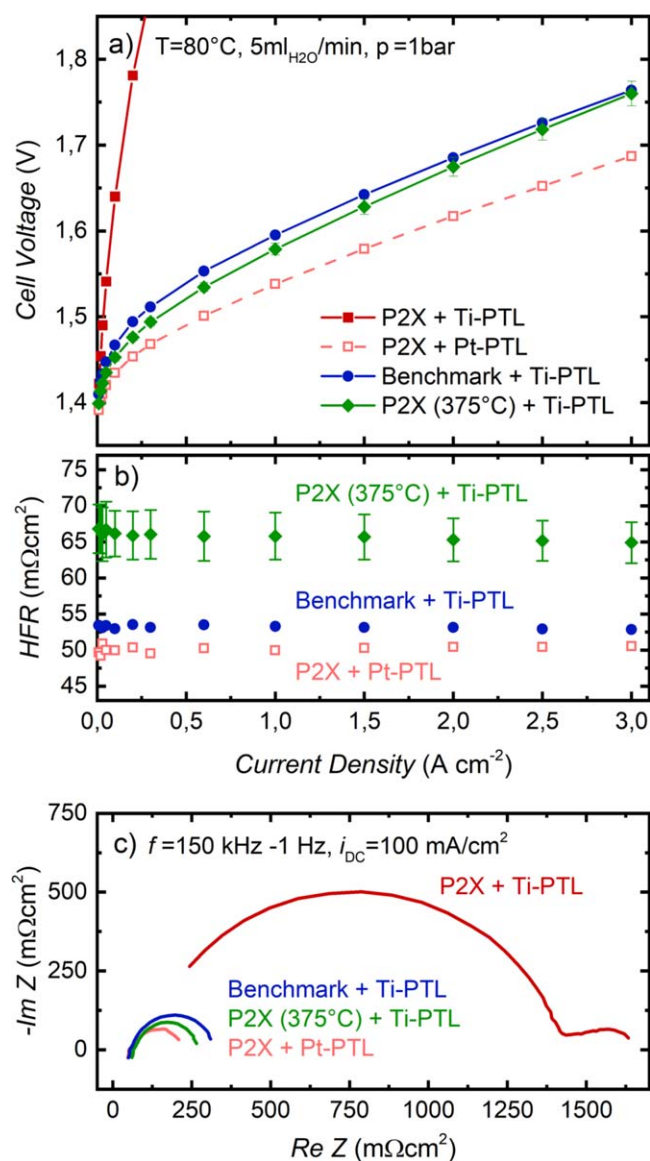
Figure 7. (a) Ambient pressure polarization curves at 80 °C measured for a 5 cm² single-cell PEM-WE with MEAs using the Benchmark catalyst in combination with a Ti-PTL (dark blue, full symbols) and the untreated P2X catalyst in combination with a Ti-PTL (dark red, full symbols) or a Pt-PTL (light red, open symbols). The green curve along with the full symbols represents the average of three MEAs employing the P2X catalyst heat-treated in O₂ at 375 °C (P2X (375 °C)) in combination with a Ti-PTL. (b) Corresponding HFR-values vs current density obtained by electrochemical impedance spectroscopy. (c) Nyquist plot of impedance measurements (i_{DC} = 0.1 A cm⁻², i_{AC} = 0.012 A cm⁻², f = 150 kHz–1 Hz) for the Benchmark catalyst in combination with a Ti-PTL (blue), for the P2X catalyst in combination with a Ti-PTL (dark red), for the P2X catalyst in combination with a platinized PTL (light red), as well as for the heat-treated P2X (375 °C) catalyst in combination with a Ti-PTL (green). MEA specifications: Nafion® 212 membrane; cathode catalyst loading of ≈0.38 mg$_{Pt}$ cm⁻²; anode catalyst loadings of ≈2.33 mg$_{Ir}$ cm⁻² for the Benchmark catalyst and ≈0.27 mg$_{Ir}$ cm⁻² for the untreated and the heat-treated P2X catalyst.

catalyst is still significantly higher compared to the Benchmark catalyst, allowing for a lower iR-free cell voltage even at a significantly lower Ir loading (≈0.27 mg$_{Ir}$ cm⁻² for P2X (375 °C) vs ≈2.33 mg$_{Ir}$ cm⁻² for Benchmark; cf Fig. 6). In the following section, we will discuss how the higher conductivity of the P2X (375 °C) catalyst after the heat treatment affects the cell performance in combination with an untreated Ti-PTL.

Cell performance of the P2X catalyst heat-treated at 375 °C.— The goal of the heat treatment of the P2X catalyst was to increase its electrical conductivity to a level sufficient to avoid the formation of a contact resistance at the electrode/PTL interface when using a Ti-PTL and, hence, rendering a Pt coating of the PTL unnecessary. Consequently, MEAs based on the P2X (375 °C) catalyst were tested in combination with an untreated Ti-PTL and the results are compared to MEAs based on the untreated P2X catalyst as well as the Benchmark catalyst (cf Fig. 7). While the Benchmark catalyst shows a good performance (blue curve in Fig. 7a) along with a low HFR (blue circles in Fig. 7b) even in combination with a Ti-PTL (same data as in Fig. 2), the untreated P2X catalyst only reaches a high performance when it is combined with a platinized PTL (light red curve in Fig. 7a; again, the same data as in Fig. 2). If an untreated Ti-PTL is used, a large contact resistance forms at the electrode/PTL interface (cf large semicircle in the Nyquist plot, dark red curve in Fig. 7c) leading to an overall poor performance (dark red curve in Fig. 7a) as already discussed before for Fig. 2. On the other hand, after the heat treatment, the P2X (375 °C) catalyst in combination with an untreated Ti-PTL (green curve in Fig. 7a) shows a similar performance compared to the Benchmark catalyst, reaching an essentially identical cell voltage of ≈1.76 V at 3 A cm⁻². This proves that the contact resistance at the electrode/PTL interface leading to a poor performance for the untreated P2X catalyst could be reduced significantly by the heat treatment in O₂ at 375 °C and the associated ≈100-fold increase in catalyst conductivity.

This is further confirmed by the Nyquist plot clearly showing the absence of a second semicircle related to a contact resistance for the P2X (375 °C) catalyst (green line in Fig. 7c). However, the performance of the P2X (375 °C) catalyst in combination with a Ti-PTL is still lower than for the untreated P2X catalyst with a Pt-PTL (light red curve in Fig. 7a) which exhibits a ≈0.07 V lower cell voltage of only ≈1.69 V at 3 A cm⁻² at the same iridium loading of ≈0.27 mg$_{Ir}$ cm⁻². This performance difference can be explained partly by the lower activity of the P2X catalyst after the heat treatment (167 A g$_{Ir}$⁻¹ vs 440 A g$_{Ir}$⁻¹ at an iR-free cell voltage of 1.43 V), but particularly at the higher current densities this difference is mostly due to a higher *HFR* (65.8 ± 3.9 mΩcm²) compared to the untreated P2X catalyst in combination with a Pt-PTL (50.1 ± 0.9 mΩcm²), which is responsible for a ≈47 mV higher ohmic voltage loss at 3 A cm⁻² (i.e., $i \cdot \Delta HFR \approx 47$ mV). In general, a difference in *HFR* is not surprising, since the usage of a platinized PTL will always result in a lower contact resistance at the electrode/PTL interface and, hence, in a lower *HFR* (assuming a similar membrane resistance for both MEAs). In fact, when a platinized PTL was used the *HFR* was in a range of 47 ± 5 mΩcm² for all tested samples, which is within the typical error range of a *HFR* measurement. This means that the *HFR* and, hence, the electric contact resistance is essentially independent of catalyst powder conductivity, which varies between 0.7–416 S cm⁻¹ for the different catalysts, when a platinized PTL is used. However, when an untreated Ti-PTL is used, the *HFR* of the Benchmark catalyst is significantly lower (53.1 ± 0.5 mΩcm²) compared to the P2X (375 °C) catalyst (65.8 ± 3.9 mΩcm²). This shows that the lower electrical conductivity of the P2X (375 °C) catalyst (67 S cm⁻¹) compared to the Benchmark catalyst (416 S cm⁻¹) results in a ≈13 mΩcm² increase of the electrode/PTL contact resistance with the untreated Ti-PTL. For the P2X catalyst heat-treated at 330 °C the conductivity is slightly lower compared to the P2X (375 °C) catalyst at 38 S cm⁻¹ resulting in an HFR of ≈110 mΩcm² (data not shown). This indicates that even moderate changes of the catalyst conductivity can have a significant effect on the electric contact resistance when using an untreated Ti-PTL. In comparison to the Benchmark catalyst, the P2X (375 °C) catalyst suffers from a ≈39 mV higher ohmic voltage loss at 3 A cm⁻² due to its higher electric contact resistance. However, this increase of the ohmic overpotential is compensated by the higher mass activity of the P2X (375 °C) catalyst compared to the Benchmark catalyst, so that a similar cell voltage of ≈1.76 V at 3 A cm⁻² is obtained. This is a very promising result, since the iridium loading is

significantly lower for the P2X (375 °C) catalyst ($\approx$0.27 mg_{Ir} cm^{-2}) compared to the Benchmark catalyst ($\approx$2.33 mg_{Ir} cm^{-2}) and shows that the P2X (375 °C) catalyst can provide high performance at very low Ir loadings even in combination with an untreated Ti-PTL. The ohmic overpotential penalty for the P2X (375 °C) catalyst may be reduced for a higher nominal iridium oxide film thickness which, however, would result in a lower iridium utilization and thus a proportionally lower mass activity (e.g., doubling the nominal iridium oxide film thickness by a factor of 2 is expected to lead to a $\approx$15 mV higher OER overpotential ($\equiv \log 2 \cdot$ Tafel slope)).

Conclusions

In this study, we compared a commercial crystalline IrO_2/TiO_2 "Benchmark" catalyst (75 wt% Ir, from Umicore) to a newly developed amorphous $IrO(OH)_x/TiO_2$ catalyst (45 wt% Ir, from Heraeus Deutschland, referred to as "P2X" catalyst) by studying the MEA performance (based on a Pt/C cathode, and a Nafion® 212 membrane) in a 5 cm^2 single-cell PEM water electrolyzer in combination with different anode PTLs. The influence of a heat treatment under O_2 on the properties of the P2X catalyst was discussed in terms of its electrical conductivity, OER mass activity, and the resulting MEA performance.

First, the MEA performance of the untreated P2X catalyst was compared to the Benchmark catalyst. Due to its lower Ir content, the P2X catalyst exhibits a lower Ir packing density ($\approx$0.5 g_{Ir} cm^{-3}) compared to the Benchmark catalyst ($\approx$2.3 g_{Ir} cm^{-3}), allowing for a significant reduction of the Ir loading while maintaining a sufficient electrode thickness. Additionally, the low Ir content and the amorphous nature of the $IrO(OH)_x$ result in a higher mass activity (440 A g_{Ir}^{-1} at 1.43 $V_{iR-free}$) but a lower electrical conductivity (0.7 S cm^{-1}) compared to the Benchmark catalyst (12 A g_{Ir}^{-1}; 416 S cm^{-1}). This leads to an improved MEA performance for the P2X catalyst ($\approx$1.69 V at 3 A cm^{-2}) at a $\approx$9 times reduced Ir loading compared to the Benchmark catalyst ($\approx$1.74 V at 3 A cm^{-2}), however, only if a platinized titanium PTL (Pt-PTL) is used. While the performance of the MEAs with the Benchmark catalyst is almost not affected when using non-platinized titanium PTL (Ti-PTL), the low electrical conductivity of the P2X catalyst combined with the passivated surface of the Ti-PTL leads to the formation of a large contact resistance at the electrode/PTL interface, resulting in a poor MEA performance.

In order to improve the conductivity of the P2X catalyst by transforming the amorphous $IrO(OH)_x$ into a crystalline IrO_2, a heat treatment at temperatures of 330 °C–390 °C was applied. An optimum was found at 375 °C, resulting in a $\approx$100-fold increase of the electrical conductivity to 67 S cm^{-1}, while the OER mass activity decreased by only $\approx$2.5-fold (167 A g_{Ir}^{-1}) compared to the untreated P2X catalyst. This increase in catalyst conductivity resulted in significant reduction of the electrode/PTL contact resistance for the P2X (375 °C) catalyst in combination with a Ti-PTL, leading to a similar performance compared to the Benchmark catalyst with $\approx$1.76 V at 3 A cm^{-2}, even though the Ir loading for the P2X (375 °C) catalyst ($\approx$0.27 mg_{Ir} cm^{-2}) was $\approx$8-fold lower compared to that of the Benchmark catalyst ($\approx$2.33 mg_{Ir} cm^{-2}). An even further reduction of the Ir packing density and, hence, the Ir loading could in principal be achieved with the same catalyst design concept by integrating TiO_2 support materials with a lower surface area in the future.

Acknowledgments

Data Availability Statement

N.A.

ORCID

M. Bernt https://orcid.org/0000-0001-8448-5532
J. Schröter https://orcid.org/0000-0001-7114-8502
H. A. Gasteiger https://orcid.org/0000-0001-8199-8703

References

1. M. Carmo, D. L. Fritz, J. Mergel, and D. Stolten, *Int. J. Hydrogen Energy*, **38**, 4901 (2013).
2. L. Bertuccioli, A. Chan, D. Hart, F. Lehner, B. Madden, and E. Standen, *Study on development of water electrolysis in the EU, Final Report*, Cambridge, UK (2014), www.fch.europa.eu/sites/default/files/FCHJUElectrolysisStudy_FullReport%20(ID%20199214).pdf.
3. A. Buttler and H. Spliethoff, *Renew. Sustain. Energy Rev.*, **82**, 2440 (2018).
4. K. Ayers, N. Danilovic, R. Ouimet, M. Carmo, B. Pivovar, and M. Bornstein, *Annual Review of Chemical and Biomolecular Engineering*, **10**, 219 (2019).
5. U. Babic, M. Suermann, F. N. Büchi, L. Gubler, and T. J. Schmidt, *J. Electrochem. Soc.*, **164**, F387 (2017).
6. M. Bernt, A. Siebel, and H. A. Gasteiger, *J. Electrochem. Soc.*, **165**, F305 (2018).
7. M. Bernt, A. Hartig-Weiß, M. F. Tovini, H. A. El-Sayed, C. Schramm, J. Schröter, C. Gebauer, and H. A. Gasteiger, *Chem. Ing. Tech.*, **92**, 31 (2020).
8. M. Miles, E. Klaus, B. Gunn, J. Locker, W. Serafin, and S. Srinivasan, *Electrochim. Acta*, **23**, 521 (1978).
9. I. C. Man, H. Y. Su, F. Calle-Vallejo, H. A. Hansen, J. I. Martínez, N. G. Inoglu, J. Kitchin, T. F. Jaramillo, J. K. Nørskov, and J. Rossmeisl, *ChemCatChem*, **3**, 1159 (2011).
10. S. Cherevko, S. Geiger, O. Kasian, N. Kulyk, J.-P. Grote, A. Savan, B. R. Shrestha, S. Merzlikin, B. Breitbach, and A. Ludwig, *Catal. Today*, **262**, 170 (2016).
11. S. Siracusano, N. Van Dijk, E. Payne-Johnson, V. Baglio, and A. Aricò, *Appl. Catalysis B*, **164**, 488 (2015).
12. O. Kasian, S. Geiger, P. Stock, G. Polymeros, B. Breitbach, A. Savan, A. Ludwig, S. Cherevko, and K. J. Mayrhofer, *J. Electrochem. Soc.*, **163**, F3099 (2016).
13. C. Spöri, P. Briois, H. N. Nong, T. Reier, A. Billard, S. Kühl, D. Teschner, and P. Strasser, *ACS Catal.*, **9**, 6653 (2019).
14. T. Reier, D. Teschner, T. Lunkenbein, A. Bergmann, S. Selve, R. Kraehnert, R. Schlögl, and P. Strasser, *J. Electrochem. Soc.*, **161**, F876 (2014).
15. S. Geiger, O. Kasian, B. R. Shrestha, A. M. Mingers, K. J. Mayrhofer, and S. Cherevko, *J. Electrochem. Soc.*, **163**, F3132 (2016).
16. H. N. Nong, H. S. Oh, T. Reier, E. Willinger, M. G. Willinger, V. Petkov, D. Teschner, and P. Strasser, *Angew. Chem. Int. Ed.*, **54**, 2975 (2015).
17. F. Godínez-Salomón, L. Albiter, S. M. Alia, B. S. Pivovar, L. E. Camacho-Forero, P. B. Balbuena, R. Mendoza-Cruz, M. J. Arellano-Jimenez, and C. P. Rhodes, *ACS Catal.*, **8**, 10498 (2018).
18. S. M. Alia, S. Shulda, C. Ngo, S. Pylypenko, and B. S. Pivovar, *ACS Catal.*, **8**, 2111 (2018).
19. Q. Feng, G. Liu, B. Wei, Z. Zhang, H. Li, and H. Wang, *J. Power Sources*, **366**, 33 (2017).
20. S. Sun, Z. Shao, H. Yu, G. Li, and B. Yi, *J. Power Sources*, **267**, 515 (2014).
21. T. Schuler, J. M. Ciccone, B. Krentscher, F. Marone, C. Peter, T. J. Schmidt, and F. N. Büchi, *Adv. Energy Mater.*, **10**, 1903216 (2020).
22. F. Hegge, F. Lombeck, E. Cruz Ortiz, L. Bohn, M. von Holst, M. Kroschel, J. Hübner, M. Breitwieser, P. Strasser, and S. Vierrath, *ACS Appl. Energy Mater.*, **3**, 8276 (2020).
23. G. Lodi, A. De Battisti, G. Bordin, C. De Asmundis, and A. Benedetti, *J. Electroanal. Chem. Interfacial Electrochem.*, **277**, 139 (1990).
24. E. Rasten, G. Hagen, and R. Tunold, *Electrochim. Acta*, **48**, 3945 (2003).
25. F. Wagner, S. Yan, and P. Yu, *Handbook of Fuel Cells*, ed. W. Vielstich, H. A. Gasteiger, and H. Yokokama (Wiley, New York, NY) 5, 250 (2009).
26. T. Y. Paul, W. Gu, J. Zhang, R. Makharia, F. T. Wagner, and H. A. Gasteiger, *Polymer Electrolyte Fuel Cell Durability* (Springer, Berlin)29 (2009).
27. D. Böhm, M. Beetz, M. Schuster, K. Peters, A. G. Hufnagel, M. Döblinger, B. Böller, T. Bein, and D. Fattakhova-Rohlfing, *Adv. Funct. Mater.*, **30**, 1906670 (2020).
28. H. S. Oh, H. N. Nong, and P. Strasser, *Adv. Funct. Mater.*, **25**, 1074 (2015).
29. V. Müller, M. Rasp, J. Rathouský, B. Schütz, M. Niederberger, and D. Fattakhova-Rohlfing, *Small*, **6**, 633 (2010).
30. V. Skoromets, H. Němec, J. Kopeček, P. Kužel, K. Peters, D. Fattakhova-Rohlfing, A. Vetushka, M. Müller, K. Ganzerová, and A. Fejfar, *The Journal of Physical Chemistry C*, **119**, 19485 (2015).
31. A. Hartig-Weiss, M. Miller, H. Beyer, A. Schmitt, A. Siebel, A. T. S. Freiberg, H. A. Gasteiger, and H. A. El-Sayed, *ACS Appl. Nano Mater.*, **3**, 2185 (2020).
32. Y. Liu, J. M. Szeifert, J. M. Feckl, B. Mandlmeier, J. Rathousky, O. Hayden, D. Fattakhova-Rohlfing, and T. Bein, *ACS Nano*, **4**, 5373 (2010).

33. H. Xu, *High-Performance, Long-Lifetime Catalysts for Proton Exchange Membrane Electrolysis*, DOE Hydrogen and Fuel Cells Program, Annual Progress Report (2016).
34. G. Auer, P. Woditsch, A. Westerhaus, J. Kischkewitz, W. D. Griebler, M. Rohe, and M. Liedekerke, *Ullmann's Encyclopedia of Industrial Chemistry* (Wiley, Weinheim) 1 (2000).
35. R. E. Fuentes, J. Farell, and J. W. Weidner, *Electrochem. Solid-State Lett.*, **14**, E5 (2011).
36. E. Oakton, D. Lebedev, A. Fedorov, F. Krumeich, J. Tillier, O. Sereda, T. J. Schmidt, and C. Copéret, *New J. Chem.*, **40**, 1834 (2016).
37. M. Lopez and A. Schleunung, *Precious Metal Oxide Catalyst for Water Electrolysis, EU Patent EP*, 1 701 790 B1 (2009).
38. M. Bernt and H. A. Gasteiger, *J. Electrochem. Soc.*, **163**, F3179 (2016).
39. Y. N. Regmi, E. Tzanetopoulos, G. Zeng, X. Peng, D. I. Kushner, T. A. Kistler, L. A. King, and N. Danilovic, *ACS Catal.*, **10**, 13125 (2020).
40. H. Beyer, M. Metzger, J. Sicklinger, X. Wu, K. U. Schwenke, and H. A. Gasteiger, *J. Electrochem. Soc.*, **164**, A1026 (2017).
41. Kopernikus P2X project funded by the German Ministry of Education and Research (BMBF), (https://kopernikus-projekte.de/en/projects/power2x) (accessed 06/29/2019).
42. D. Böhm, M. Beetz, C. Gebauer, M. Bernt, J. Schröter, M. Kornherr, F. Zoller, T. Bein, and D. Fattakhova-Rohlfing, *Appl. Mater. Today*, **24**, 101134 (2021).
43. W. Gu, D. R. Baker, Y. Liu, and H. A. Gasteiger, *Handbook of Fuel Cells*, ed. W. Vielstich, H. A. Gasteiger, and H. Yokokama (Wiley, Chichester, UK) 6, 631 (2009).
44. M. Gaberscek, J. Moskon, B. Erjavec, R. Dominko, and J. Jamnik, *Electrochem. Solid-State Lett.*, **11**, A170 (2008).
45. J. Landesfeind, J. Hattendorff, A. Ehrl, W. A. Wall, and H. A. Gasteiger, *J. Electrochem. Soc.*, **163**, A1373 (2016).
46. A. Weiß, A. Siebel, M. Bernt, T.-H. Shen, V. Tileli, and H. A. Gasteiger, *J. Electrochem. Soc.*, **166**, F487 (2019).
47. F. Karimi, A. Bazylak, and B. A. Peppley, *J. Electrochem. Soc.*, **164**, F464 (2017).